



## Full Length Article

## Laminar flame speeds of lean high-hydrogen syngas at normal and elevated pressures

Weikuo Zhang<sup>a,b</sup>, Xiaolong Gou<sup>a,\*</sup>, Wenjun Kong<sup>c</sup>, Zheng Chen<sup>b,a</sup><sup>a</sup>Key Laboratory of Low-grade Energy Utilization Technologies and Systems, School of Power Engineering, Chongqing University, Chongqing 400044, China<sup>b</sup>SKLTCS, Department of Mechanics and Engineering Science, College of Engineering, Peking University, Beijing 100871, China<sup>c</sup>Institute of Engineering Thermophysics, Chinese Academy of Sciences, Beijing 100190, China

## HIGHLIGHTS

- Laminar flame speeds of lean high-hydrogen syngas were measured.
- A broad range of pressure from 1 atm to 10 atm was considered.
- The performances of three syngas mechanisms were examined.
- Good agreement between simulation and experiments was achieved.

## ARTICLE INFO

## Article history:

Received 1 March 2016

Received in revised form 25 April 2016

Accepted 4 May 2016

Available online 10 May 2016

## Keywords:

Laminar flame speed

Syngas

Spherical flame

Markstein length

## ABSTRACT

The laminar flame speed is one of the most important combustion properties of a combustible mixture. It is an important target for chemical mechanism validation and development, especially at fuel-lean and high pressure conditions. In this study, the laminar flame speeds of two types of lean high-hydrogen syngas/oxygen/helium mixtures were measured at normal and elevated pressures up to 10 atm using a dual-chambered high pressure combustion facility. Similar to experiments, numerical simulations of outwardly spherical flame propagation were conducted. Three chemical mechanisms for syngas available in the literature were considered in simulation and their performance in terms of predicting the stretched flame speeds, laminar flame speeds and burned Markstein lengths was examined through comparison between experimental and simulation results. It was found that at both normal and elevated pressures, the present experimental results agree well with those predicted by simulations using these three chemical mechanisms. Therefore, these chemical mechanisms for syngas can well predict the laminar flame properties of lean high-hydrogen syngas. Besides, the laminar flame speeds measured in the present work were compared with those measured from the heat flux method and large difference was observed.

© 2016 Elsevier Ltd. All rights reserved.

## 1. Introduction

Synthesized gas (syngas) contains different amounts of CO and H<sub>2</sub> as the primary fuel components. Syngas is one of the most promising alternative fuels since it can be produced from a wide variety of sources, such as coal, biomass, and refinery residuals. Recently, syngas has received great attention due to its application in fuel-flexible gas turbine engines. Depending on the gasification sources and procedures, the composition of syngas varies widely. For example, for coal-based syngas, water–gas shift technologies can be used to generate high-hydrogen syngas. With the increase

in the hydrogen component in syngas, the combustion properties changes greatly. Therefore, high-hydrogen syngas has received great attention recently (e.g., [1–4]). Furthermore, lean syngas combustion at high pressure is promising for achieving high efficiency and low emission in gas turbine engines. Consequently, there is a need to understand fundamental combustion properties of lean high-hydrogen syngas at elevated pressures. In this study, the laminar flame speeds of lean high-hydrogen syngas at elevated pressures were investigated experimentally and numerically.

The laminar flame speed,  $S_L$ , is one of the most important properties of a combustible mixture. It determines the burning rate and flame stabilization in engines. Moreover, it is also an important target for validating chemical mechanisms. Therefore, in the literature there are many studies [1–15] on the laminar flame speed of

\* Corresponding author.

E-mail address: [simgxl@cqu.edu.cn](mailto:simgxl@cqu.edu.cn) (X. Gou).

syngas. For examples, Prathap et al. [2] studied the influence of carbon dioxide dilution on the laminar flame speed of syngas (50%H<sub>2</sub>–50%CO); Zhang et al. [3] studied the laminar flame speed of lean syngas/air mixtures with a broad range of hydrogen content; Sun et al. [5] studied the laminar flame speed of low-hydrogen syngas within a broad range of pressure from 1 atm to 40 atm; McLean et al. [6] measured  $S_L$  for syngas (5%H<sub>2</sub>–95%CO and 50%H<sub>2</sub>–50%CO) at atmospheric pressure; and Kong and coworkers [4,17] measured the  $S_L$  of syngas at elevated pressures and temperatures. However, most of the above studies focused on laminar flame speeds at atmospheric pressure or for fuel-rich syngas/air mixtures; and there is a scarcity of high-pressure experimental data for fuel-lean mixtures. Therefore, there is a need to investigate the laminar flame speeds of high-hydrogen syngas at elevated pressure and fuel-lean conditions.

Furthermore, substantial disparities in laminar flame speeds of syngas were observed between experimental data and model predictions at high pressures [1,5,7–9]. The difference between experimental and numerical results might be caused by the uncertainty in experimental measurement and/or the inaccuracy of chemical mechanisms. Goswami et al. [7] measured the laminar flame speeds of lean high-hydrogen syngas at elevated pressures using the heat flux method. They found that compared to experimental data, the laminar flame speeds were greatly over-predicted at elevated pressures by different syngas mechanisms [7]. Therefore, they suggested that the kinetic model for syngas needs further improvement. Since the propagating spherical flame method has the advantage in laminar flame speed measurement at high pressure, this method was used here for the same lean high-hydrogen syngas of Goswami et al. [7] at elevated pressures. Moreover, the experimental data were compared with predictions from different syngas mechanisms in the literature [19–23].

The objectives of this study are to measure laminar flame speeds of lean high-hydrogen syngas at elevated pressures up to 10 atm and to examine the performance of different syngas mechanisms in terms of predicting laminar flame speeds. The paper is organized as follows: in Section 2, the experimental and numerical methods are briefly described; then, in Section 3 the experimental and numerical results are presented together with the discussion on the performance of different syngas mechanisms; and finally, the conclusions are summarized in Section 4.

## 2. Experimental and numerical methods

We studied the same lean high-hydrogen syngas/oxygen/helium mixtures of Goswami et al. [7]: the syngas consists of 85 vol.% H<sub>2</sub> and 15 vol.% CO; and the oxidizer consists of O<sub>2</sub> and He (12.5%O<sub>2</sub>–87.5%He for  $\phi = 0.5$  and 11%O<sub>2</sub>–89%He for  $\phi = 0.6$ ). Only two mixtures for high-hydrogen syngas were considered: mixture #1 with 85%H<sub>2</sub>–15%CO/12.5%O<sub>2</sub>–87.5%He and  $\phi = 0.5$ ; and mixture #2 with 85%H<sub>2</sub>–15%CO/11%O<sub>2</sub>–89%He and  $\phi = 0.6$ . We considered the initial temperature of 298 K and a broad range of pressure from 1 atm to 10 atm. Large amount of helium was included in these mixtures so that stable spherical flame propagation can be achieved at elevated pressures [16].

The laminar flame speeds were measured from outwardly propagating spherical flames in a dual-chambered high pressure combustion facility [4,17]. Detailed description of the experimental system and procedure was presented in [4,17] and thereby only a brief description was given here. The reader is referred to Refs. [4,17] for further details. The combustion chamber consists of two concentric cylindrical chambers. Premixed mixtures were prepared inside the inner chamber (whose inner radius is  $R_w = 5$  cm and length is 15.3 cm) using the partial pressure method. The outer chamber was filled with inert gases to match the inner chamber

pressure. When the mixture was centrally spark-ignited, the spherical flame front history,  $R_f = R_f(t)$ , was recorded using high speed schlieren photography. Usually the burned gas inside the spherical flame is assumed to be static and thus the stretched flame speed relative to burned gas is  $S_b = dR_f/dt$ . The unstretched laminar flame speed,  $S_b^0$ , and Markstein length,  $L_b$ , both relative to burned gas, can be obtained from extrapolation based on the following linear relationship:

$$S_b = S_b^0 - L_b K \quad (1)$$

where  $K = (2/R_f)(dR_f/dt)$  is the stretch rate of outwardly propagating spherical flames. Finally, the laminar flame speed  $S_L$  is calculated from  $S_L = \sigma S_b^0$ , in which  $\sigma$  is the ratio between burned gas density and unburned gas density. It is noted that there are different linear and nonlinear extrapolations as reported in [24,25]. Wu et al. [25] demonstrated a failure of the linear stretch correction for lean hydrogen flames with systematic over prediction up to 60%. In this study, the effective Lewis number of mixtures #1 and #2 is close to unity and the magnitude of burned Markstein length is within 1 mm. Therefore, the nonlinear behavior is not strong [25] and in fact we found the stretched flame speed changes linearly with the stretch rate for the flame radius range considered in this work (see results shown later). Therefore, the linear extrapolation was used here. Besides, the nonlinear extrapolations might induce large uncertainty in laminar flame speed measurement [26].

The uncertainties of experimental data may come from several sources [34] such as ignition, flame instability, radiation and extrapolation. In the present work, these sources bring little uncertainty for mixtures #1 and #2 and the main source are the uncertainty in the experimental uncertainty ( $\delta_{S_L}$ ) and equivalence ratio ( $\phi$ ). The method of analyzing experimental uncertainty for the  $S_L$  measurement was proposed by Moffat [39], and  $\delta_{S_L}$  can be estimated by the following equation:

$$\delta_{S_L} = \sqrt{(B_{S_L})^2 + [t_{1-\alpha/2}(\nu)\sigma_{S_L}]^2} \quad (2)$$

where  $B_{S_L}$  is the total bias uncertainty and in this study  $B_{S_L}$  is estimated to be about  $\pm 0.9$  cm/s, because  $S_L$  was determined by the linear extrapolation.  $t_{1-\alpha/2}$  is the student  $t$  value at 95% confidence interval and  $\nu$  is the degree of freedom, in present experiments  $\nu$  is estimated to be 12–25.  $\sigma_{S_L}$  is the standard deviation of representing  $S_L$  random uncertainties caused by the initial temperature fluctuation and radiation, etc., here  $\sigma_{S_L}$  was estimated to be about 0.6–1.2 cm/s. From Eq. (2),  $\delta_{S_L}$  was estimated to be about  $\pm 1.5$ –2.8 cm/s. The uncertainty in the equivalence ratio was about  $\pm 2\%$ . And our estimation indicated that the overall uncertainty in the laminar flame speed was within  $\pm 5\%$ .

Besides experiments, the outwardly propagating spherical flames for lean high-hydrogen syngas were simulated using the in house code A-SURF [27–29]. A-SURF solves the conservation equations for a multi-component reactive flow using the finite volume method. A-SURF was used in previous studies on ignition and spherical flame propagation (e.g., [30–34]). The reader is referred to [27–29] for details on governing equations, numerical methods and code validation of A-SURF. In all simulations, the spherical chamber radius was  $R_w = 100$  cm and only flame radius between 0.75 cm and 1.25 cm was utilized for data processing. Consequently, the ignition effects [27,35] and compression effects [28,31] were both negligible. At the initial state, the homogeneous mixture was quiescent at 298 K and specified pressure. Zero flow speed and zero gradients of temperature and mass fractions were enforced at both the center and wall boundaries. Flame initiation was achieved by spatial-dependent energy deposition within a given time period and a given ignition kernel size [31]. In order to adequately resolve the moving flame front, a multilevel, dynamically adaptive mesh was employed and the propagating reaction

front was always covered by smallest mesh size of 8  $\mu\text{m}$ . Different chemical mechanisms for syngas developed by Davis et al. [18], Li et al. [19] and K eromn es et al. [20] were used in simulations. Besides, the one-dimensional, steady, adiabatic, freely-propagating planar flame was simulated using the CHEMKIN-PREMIX Code [37] to get  $S_L$  and  $\sigma$  [29,31]. The same chemical mechanism and transport properties were used for both PREMIX and A-SURF so that consistent results were obtained.

### 3. Results and discussion

As mentioned before, two mixtures for high-hydrogen syngas [7] were considered: mixture #1 with 85% $\text{H}_2$ –15% $\text{CO}$ /12.5% $\text{O}_2$ –87.5% $\text{He}$  and  $\phi = 0.5$ ; and mixture #2 with 85% $\text{H}_2$ –15% $\text{CO}$ /11% $\text{O}_2$ –89% $\text{He}$  and  $\phi = 0.6$ . Due to space limit, the photographic images of outwardly propagating spherical flames were presented in the [Supplementary Material](#).

Fig. 1 shows the measured stretch flame speed  $S_b$  versus stretch rate  $K$  for mixture #1 at different pressures of  $P = 1, 2, 4, 6, 8$  and 10 atm. During spherical flame propagation, the stretch rate decreases since it is proportional to the inverse of flame radius. When the flame radius is above a value around 1.5 cm, the flame propagation speed decreases due to the confinement effects [28,31,36]. This is indicated by the fact that  $S_b$  decreases as  $K$  decreases at small stretch rate, as shown in Fig. 1. Moreover, the spherical flame propagation can be affected by ignition and unsteady transition [27,35]. Therefore, the experimental data range of  $0.75 \leq R_f \leq 1.25$  cm (the read open symbols in Fig. 1) was used for linear extrapolation of  $S_b^0$  and  $L_b$  based on Eq. (1). Fig. 1 indicates that the linear behavior between  $S_b$  and  $K$  maintains for  $0.75 \leq R_f \leq 1.25$  cm. Therefore, the linear model in Eq. (1) is appropriate for the extrapolation of unstretched flame speed and Markstein length.

Fig. 2 compares  $S_b$  versus  $K$  predicted by three different syngas mechanisms. It is observed that  $S_b$  predicted by the mechanism of K eromn es et al. [20] is always the highest while that by the mechanism of Davis et al. [18] is the smallest. Nevertheless, the flame speeds predicted by these three syngas mechanisms are very close: the relative difference is within 10%. Besides, Fig. 2 also shows the unstretched flame speeds relative to burned gas,  $S_b^0$ , predicted by CHEMKIN-PREMIX code based on 1D unstretched planar flame (the closed symbols at zero stretched rate). It is seen that the results from PREMIX are in good agreement with those from linear extrapolation of spherical flame results predicted by A-SURF. This

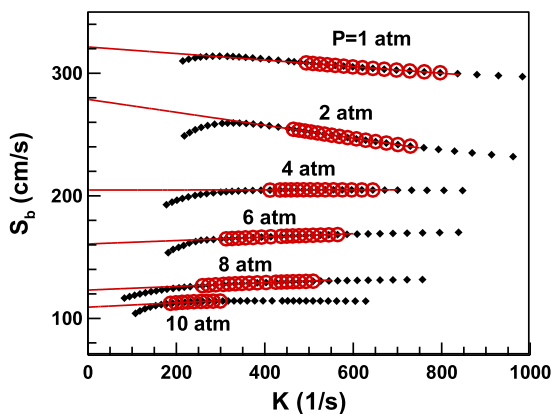


Fig. 1. Measured stretched flame speed as a function of stretch rate for mixture #1 with 85% $\text{H}_2$ –15% $\text{CO}$ /12.5% $\text{O}_2$ –87.5% $\text{He}$  and  $\phi = 0.5$ . The closed symbols denote experimental data; the open symbols are data used for linear fitting with the flame radius from 0.75 cm to 1.25 cm; and the solid lines stand for linear fitting.

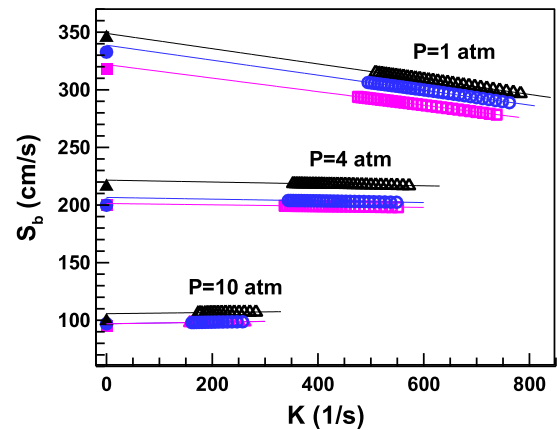


Fig. 2. Calculated stretched flame speed as a function of stretch rate for mixture #1 at  $P = 1, 4, 10$  atm. These results were from simulations using different chemical mechanisms: triangles, K eromn es et al. [20]; circles, Li et al. [19]; squares, Davis et al. [18]. The open symbols are results from A-SURF for spherical flames with radius from 0.75 cm to 1.25 cm; the solid lines stand for linear fitting; and the closed symbols denote results from PREMIX.

indicates the validity of the A-SURF simulation in terms of calculating laminar flame speeds.

The comparison between experimental results and those predicted by different mechanisms is shown in Figs. 3 and 4. Fig. 3 plots the measured and calculated stretched flame speeds versus stretch rate for mixture #1 at  $P = 1, 4, 10$  atm. Only the simulation

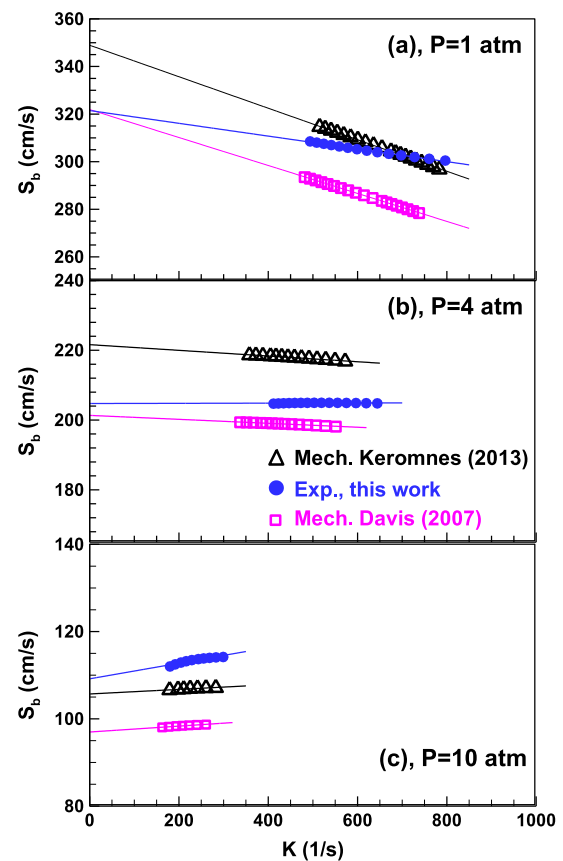


Fig. 3. Measured (closed symbols) and calculated (open symbols) stretched flame speeds as a function of stretch rate for mixture #1 at  $P = 1, 4, 10$  atm. The solid lines stand for linear extrapolation.

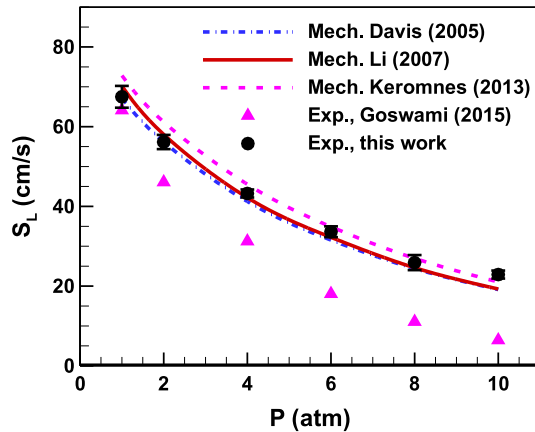


Fig. 4. Laminar flame speed of mixture #1 as a function of pressure. The lines are simulation results based on different syngas mechanisms; and the symbols are experimental results.

results based on the mechanisms of K eromn es et al. [20] and Davis et al. [18] are shown since they respectively provide the highest and the lowest stretched flame speeds as shown in Fig. 2. Fig. 3 does indicate that there are discrepancies between stretched flame speeds measured in experiments and those predicted by different chemical mechanisms. Nevertheless, the relative difference is still within 10%, which is close to or even smaller than the relative difference among predictions from different chemical mechanisms.

Fig. 4 plots the laminar flame speeds of mixture #1 measured in this work and those measured by Goswami et al. [7] for a broad range of pressure from 1 atm to 10 atm. The predictions from three different mechanisms are shown together for comparison. It is seen that the laminar flame speed monotonically decreases as the pressure increases. This is reasonable since  $S_L \sim p^{(n/2-1)}$  and the overall reaction order  $n$  is usually less than 2 due to the third-body, inhibiting reaction  $H + O_2 + M \rightarrow HO_2 + M$  [38]. Moreover, Fig. 4 demonstrates that there is close agreement between present experimental data and predictions from three chemical mechanisms of Davis et al. [18], Li et al. [19], and K eromn es et al. [20] though the prediction of K eromn es et al. [20] is slightly higher than other data. However, the experimental data measured from heat flux method by Goswami et al. [7] are shown to be substantially lower than the present experimental data and those predicted by three chemical mechanisms. It is shown that the difference between experimental data of the present work and those from Goswami et al. [7] increases greatly with the pressure: the relative difference reaches around 70% for  $P = 10$  atm. Such large difference makes experimental data unhelpful for restraining the uncertainty in chemical mechanisms. Unfortunately, the source of such disagreement between laminar flame speed measurements using two different methods (propagating spherical flame method and heat flux method) is not clear and it is a question for further study.

To further demonstrate the influence of pressure on stretched flame propagation, the Markstein length  $L_b$  was obtained. Fig. 5 shows the burned Markstein length  $L_b$ , as a function of pressure for mixture #1. Both numerical and experimental results are shown to decrease with the pressure. When the pressure is above 5 atm, the burned Markstein length becomes negative and the flame propagation is affected by the diffusion-thermal instability. However, for flames with small radii, the large positive stretch stabilizes the spherical flame propagation. For  $1 \leq P \leq 5$  atm, the Markstein length is shown to be very sensitive to pressure. This is due to the strong dependence of flame thickness on pressure. Besides, Fig. 5 also shows that the burned Markstein lengths measured in present work agree well with those from simulation at

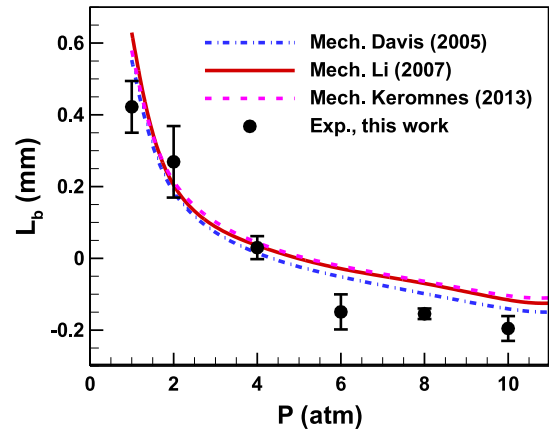


Fig. 5. Burned Markstein length of mixture #1 as a function of pressure. The lines are simulation results based on different syngas mechanism; and the symbols are experimental results.

least for low pressures. It is noted that the uncertainty in Markstein length measurement is about one-order higher than that in laminar flame speed measurement [24].

Similarly, we also conducted experiments and simulations for mixture #2 initially at 298 K and different pressures of  $P = 1, 2, 3, 4, 5, 8$  and 10 atm. The results are shown in Figs. 6–9. Fig. 6 demonstrates that the linear behavior between  $S_b$  and  $K$  maintains for experimental spherical flames with  $0.75 \leq R_f \leq 1.25$  cm. Therefore, linear extrapolation of  $S_b^0$  and  $L_b$  based on Eq. (1) can be used for experimental data processing. Fig. 7 compares the stretched flame speeds measured from experiments with those from simulations using two chemical mechanisms. Similar to Fig. 3, Fig. 7 shows that the relative difference between experimental and simulation results at the same stretch rate is within 10% and thus good agreement is achieved.

The laminar flame speeds for mixture #2 are shown in Fig. 8. It is observed that good agreement between present experimental data and predictions from three chemical mechanisms is reached for  $P = 1–10$  atm. Similar to the results for mixture #1 shown in Fig. 4, Fig. 8 shows that the laminar flame speeds of mixture #2 measured from heat flux method by Goswami et al. [7] are much lower than the present experimental data and those predicted by three chemical mechanisms. The relative difference between

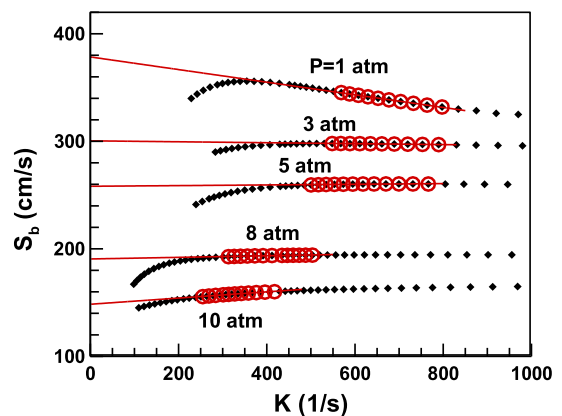


Fig. 6. Measured stretched flame speed as a function of stretch rate for mixture #2 with 85% $H_2$ –15% $CO$ /11% $O_2$ –89% $He$  and  $\phi = 0.6$ . The closed symbols denote experimental data; the open symbols are data used for linear fitting with the flame radius from 0.75 cm to 1.25 cm; and the solid lines stand for linear fitting.

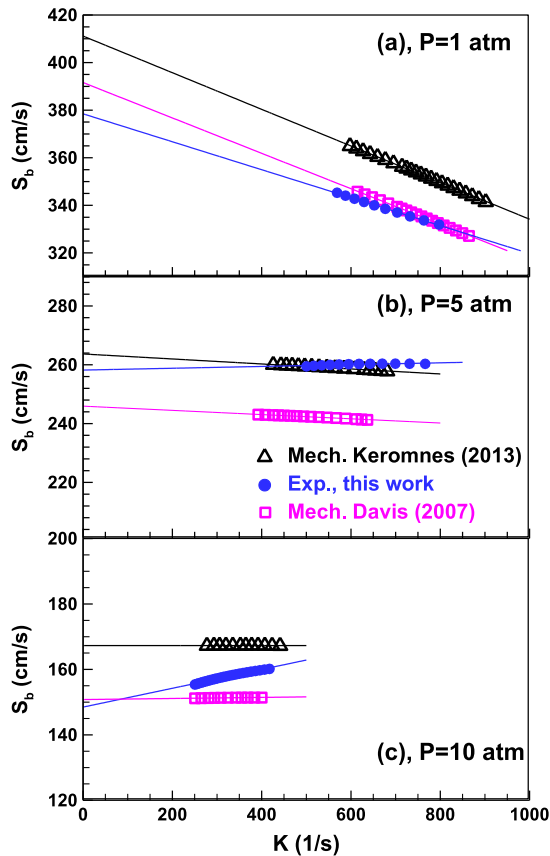


Fig. 7. Measured (closed symbols) and calculated (open symbols) stretched flame speeds as a function of stretch rate for mixture #2 at  $P=1, 5, 10$  atm. The solid lines stand for linear extrapolation.

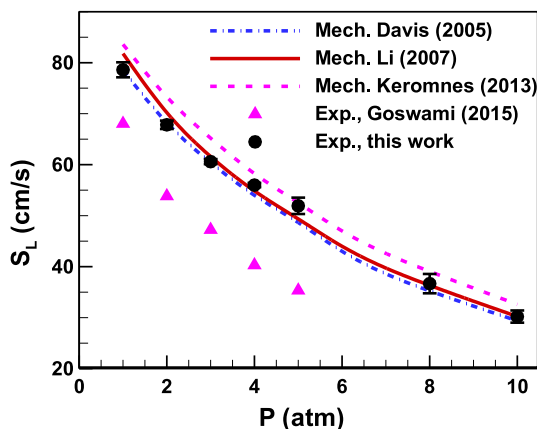


Fig. 8. Laminar flame speed of mixture #2 as a function of pressure. The lines are simulation results based on different syngas mechanisms; and the symbols are experimental results.

experimental data of the present work and those from Goswami et al. [7] increases significantly with the pressure: the relative difference reaches around 40% for  $P=5$  atm. Again, the source of such large disagreement needs further study.

Similar to Fig. 5, Fig. 9 shows the burned Markstein length for mixture #2 as a function of pressure. The burned Markstein length is shown to monotonically decrease with the pressure. Good agreement between experimental and simulation results is achieved except for the pressure of  $P=2$  atm.

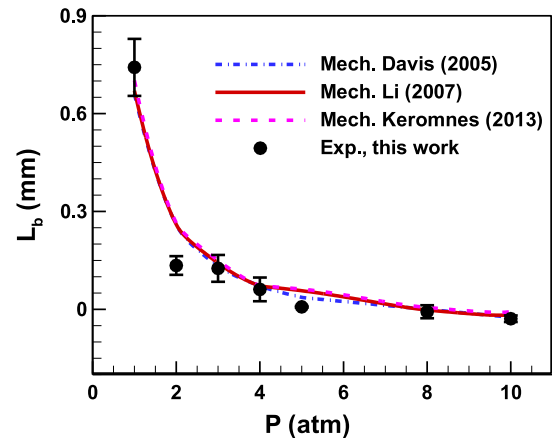


Fig. 9. Burned Markstein length of mixture #2 as a function of pressure. The lines are simulation results based on different syngas mechanism; and the symbols are experimental results.

#### 4. Conclusions

The laminar flame speeds of two types of lean high-hydrogen syngas/oxygen/helium mixtures were measured using the outwardly propagating spherical flames. The initial temperature was 298 K and a broad range of pressure from 1 atm to 10 atm was covered. Moreover, simulations were conducted for these two mixtures at the same range of initial conditions using three syngas mechanisms developed by Davis et al. [19], Li et al. [20] and K eromn es et al. [21]. It was demonstrated that the stretched flame speed changes linear with stretch rate for spherical flames with  $0.75 \leq R_f \leq 1.25$  cm. Therefore, linear extrapolation can be used to obtain the laminar flame speed and Markstein length. The stretched flame speeds, laminar flame speeds and burned Markstein lengths measured from the present experiments were shown to agree well with those predicted by simulations using these three chemical mechanisms for syngas. Good agreement was shown to maintain at both normal pressure of 1 atm and elevated pressures up to 10 atm. Therefore, these three chemical mechanisms for syngas can well predict the laminar flame properties of lean high-hydrogen syngas. This is different from the results of Goswami et al. [7] who measured the laminar flame speeds for these two mixtures and found large over-prediction by different syngas mechanisms especially at elevated pressures. For both mixtures, the laminar flame speeds measured from heat flux method by Goswami et al. [7] were much lower than the present experimental data and those predicted by three chemical mechanisms. The reason for such large difference is unclear and needs further study.

#### Acknowledgements

The work was supported by National Natural Science Foundation of China (no. 91441112). Z.C. thanks the support from Key Laboratory of Low-grade Energy Utilization Technologies and Systems at Chongqing University (no. LLEUTS 201304). We thank Mr. Minchao Han at Institute of Engineering Thermophysics for his help on experiments and Professor Yiguang Ju at Princeton University for helpful discussions.

#### Appendix A. Supplementary material

Supplementary data associated with this article can be found, in the online version, at <http://dx.doi.org/10.1016/j.fuel.2016.05.013>.

## References

- [1] Burke MP, Chaos D, Dryer FL, Ju Y. Negative pressure dependence of mass burning rates of  $H_2/CO/O_2$ /diluent flames at low flame temperatures. *Combust Flame* 2010;157:618–31.
- [2] Prathap C, Ray A, Ravi MR. Effects of dilution with carbon dioxide on the laminar burning velocity and flame stability of  $H_2$ –CO mixtures at atmospheric condition. *Combust Flame* 2012;159:482–92.
- [3] Zhang Y, Shen W, Fan M, Zhang H, Li S. Laminar flame speed studies of lean premixed  $H_2/CO$ /air flames. *Combust Flame* 2014;161:2492–5.
- [4] Han M, Ai Y, Chen Z, Kong W. Laminar flame speeds of  $H_2/CO$  with  $CO_2$  dilution at normal and elevated pressures and temperatures. *Fuel* 2015;148:32–8.
- [5] Sun H, Yang SI, Jomaas G, Law CK. High-pressure laminar flame speeds and kinetic modeling of carbon monoxide/hydrogen combustion. *Proc Combust Inst* 2007;31:439–46.
- [6] McLean IC, Smith DB, Taylor SC. The use of carbon monoxide/hydrogen burning velocities to examine the rate of the  $CO + OH$  reaction. *Proc Combust Inst* 1994;25:749–57.
- [7] Goswami M, van Griensven JGH, Bastiaans RJM, Konnov AA, de Goey LPH. Experimental and modeling study of the effect of elevated pressure on lean high-hydrogen syngas flames. *Proc Combust Inst* 2015;35:655–62.
- [8] Burke MP, Qin X, Ju Y, Dryer FL. Measurements of hydrogen syngas flame speeds at elevated pressures. In: Fifth U.S. combustion meeting, San Diego, CA, paper A16; 2007.
- [9] Li X, You X, Wu F, Law CK. Uncertainty analysis of the kinetic model prediction for high-pressure  $H_2/CO$  combustion. *Proc Combust Inst* 2015;35:617–24.
- [10] Natarajan J, Lieuwen T, Seitzman J. Laminar flame speeds of  $H_2/CO$  mixtures: effect of  $CO_2$  dilution, preheat temperature, and pressure. *Combust Flame* 2007;151:104–19.
- [11] Natarajan J, Kochar Y, Lieuwen T, Seitzman J. Pressure and preheat dependence of laminar flame speeds of  $H_2/CO/CO_2/O_2/He$  mixtures. *Proc Combust Inst* 2009;32:1261–8.
- [12] Dong C, Zhou Q, Zhao Q, Zhang Y, Xu T, Hui S. Experimental study on the laminar flame speed of hydrogen/carbon monoxide/air mixtures. *Fuel* 2009;88:1858–63.
- [13] Vagelopoulos CM, Egolfopoulos FN. Laminar flame speeds and extinction strain rates of mixtures of carbon monoxide with hydrogen, methane and air. *Proc Combust Inst* 1994;25:1317–23.
- [14] Burke MP, Chen Z, Ju Y, Dryer FL. Effect of cylindrical confinement on the determination of laminar flame speeds using outwardly propagating flames. *Combust Flame* 2009;156:771–9.
- [15] Bouvet N, Chauveau C, Gökalp I, Halter F. Experimental studies of the fundamental flame speeds of syngas ( $H_2/CO$ )/air mixtures. *Proc Combust Inst* 2011;33:913–20.
- [16] Chen Z, Qin X, Xu B, Ju Y, Liu F. Studies of radiation absorption on flame speed and flammability limit of  $CO_2$  diluted methane flames at elevated pressures. *Proc Combust Inst* 2007;31:2693–700.
- [17] Ai Y, Zhou Z, Chen Z, Kong W. Laminar flame speed and Markstein length of syngas at normal and elevated pressures and temperatures. *Fuel* 2014;137:339–45.
- [18] Davis SG, Joshi AV, Wang H, Egolfopoulos F. An optimized kinetic model of  $H_2/CO$  combustion. *Proc Combust Inst* 2005;30:1283–92.
- [19] Li J, Zhao Z, Kazakov A, Chaos M, Dryer FL. A comprehensive kinetic mechanism for  $CO$ ,  $CH_2O$ , and  $CH_3OH$  combustion. *Int J Chem Kinet* 2007;39:109–36.
- [20] Kéromnès A, Metcalfe WK, Heufer KA, Donohoe N, Das AK, Sung C, et al. An experimental and detailed chemical kinetic modeling study of hydrogen and syngas mixture oxidation at elevated pressures. *Combust Flame* 2013;160:995–1011.
- [21] Smith GP, Golden DM, Frenklach M, Moriarty NW, Eiteneer B, Goldenberg M, et al. *GRI-Mech 3.0*; 1999. <[http://www.me.berkeley.edu/gri\\_mech/](http://www.me.berkeley.edu/gri_mech/)>.
- [22] Burke MP, Chaos M, Ju Y, Dryer FL, Klippenstein SJ. Comprehensive  $H_2/O_2$  kinetic model for high-pressure combustion. *Int J Chem Kinet* 2012;44:444–74.
- [23] Goswami M, Bastiaans RJM, Konnov AA, de Goey LPH. Laminar burning velocity of lean  $H_2$ –CO mixtures at elevated pressure using the heat flux method. *Int J Hydrogen Energy* 2014;39:1485–98.
- [24] Chen Z. On the extraction of laminar flame speed and Markstein length from outwardly propagating spherical flames. *Combust Flame* 2011;158:291–300.
- [25] Wu F, Liang W, Chen Z, Ju Y, Law CK. Uncertainty in stretch extrapolation of laminar flame speed from expanding spherical flames. *Proc Combust Inst* 2015;35:663–70.
- [26] Jayachandran J, Lefebvre A, Zhao R, Halter F, Varea E, Renou B, et al. A study of propagation of spherically expanding and counterflow laminar flames using direct measurements and numerical simulations. *Proc Combust Inst* 2015;35:695–702.
- [27] Chen Z, Burke MP, Ju Y. Effects of Lewis number and ignition energy on the determination of laminar flame speed using propagating spherical flames. *Proc Combust Inst* 2009;32:1253–60.
- [28] Chen Z. Effects of radiation and compression on propagating spherical flames of methane air mixtures near the lean flammability limit. *Combust Flame* 2010;157:2267–76.
- [29] Dai P, Chen Z, Chen S, Ju Y. Numerical experiments on reaction front propagation in n-heptane/air mixture with temperature gradient. *Proc Combust Inst* 2015;35:3045–52.
- [30] Chen Z, Burke MP, Ju Y. On the critical flame radius and minimum ignition energy for spherical flame initiation. *Proc Combust Inst* 2011;33:1219–26.
- [31] Zhang W, Chen Z, Kong W. Effects of diluents on the ignition of premixed  $H_2/air$  mixtures. *Combust Flame* 2012;159:151–60.
- [32] Liang W, Chen Z, Yang F, Zhang H. Effects of Soret diffusion on the laminar flame speed and Markstein length of syngas/air mixtures. *Proc Combust Inst* 2013;34:695–702.
- [33] Zhang H, Guo P, Chen Z. Critical condition for the ignition of reactant mixture by radical deposition. *Proc Combust Inst* 2013;34:3267–75.
- [34] Chen Z. On the accuracy of laminar flame speeds measured from outwardly propagating spherical flames: methane/air at normal temperature and pressure. *Combust Flame* 2015;162:2442–53.
- [35] Bradley D, Gaskell PH, Gu XJ. Two-dimensional mathematical modeling of laminar, premixed, methane–air combustion on an experimental slot burner. *Combust Flame* 1996;26:915–21.
- [36] Chen Z, Burke MP, Ju Y. Effects of compression and stretch on the determination of laminar flame. *Combust Theory Model* 2009;13:343–64.
- [37] Kee RJ, Grcar JF, Smooke MD, Miller JA. PREMIX: a FORTRAN program for modeling steady laminar one-dimensional premixed flames. Sandia National Laboratory Report SAND85-8240; 1993.
- [38] Law CK. *Combustion physics*. 1st ed. New York: Cambridge University; 2006.
- [39] Moffat RJ. Describing uncertainties in experimental results. *Exp Therm Fluid Sci* 1988;1:3–17.